

# Pyrido[1,2-*a*]quinoxalines: synthesis, crystal structure determination and pH-dependent fluorescence †

2 PERKIN

Kevin J. Duffy,<sup>\*a</sup> R. Curtis Haltiwanger,<sup>b</sup> Alan J. Freyer,<sup>b</sup> Florence Li,<sup>b</sup> Juan I. Luengo<sup>a</sup> and Hung-Yuan Cheng<sup>b</sup>

<sup>a</sup> GlaxoSmithKline, 1250 South Collegeville Road, Collegeville, PA 19426, USA

<sup>b</sup> GlaxoSmithKline, 709 Swedeland Road, King of Prussia, PA 19406, USA

Received (in Cambridge, UK) 26th March 2001, Accepted 31st October 2001

First published as an Advance Article on the web 3rd December 2001

A series of novel, fluorescent pyrido[1,2-*a*]quinoxalines have been synthesized with crystal structures obtained for several analogues. These heterocycles exhibit characteristic pH-dependent UV-visible absorption and fluorescence properties that may be utilized for *in-situ* pH-sensing in biological experiments. The  $pK_a$  values for this series of compounds, ranging from 4.5 to 7.5, can be systematically varied by manipulating the substitutions on the quinoxaline ring. These novel fluorescent pH indicators are readily available in one synthetic step from commercially available starting materials therefore being significantly more straightforward and less expensive to synthesize than the current standard fluorescent indicators.

## Introduction

The ability of dyes such as litmus and phenolphthalein to change their color in response to a pH change has found widespread application in research and industry.<sup>1</sup> However, only fluorescent dyes can provide the greater sensitivity required for optical pH measurements inside live cells. The demand for sensitive intracellular pH indicators<sup>2</sup> has spurred the search for improved fluorescent dyes that can sense pH changes within physiological ranges. Intracellular pH is generally between ~6.8 and 7.4 in the cytosol and ~4.5 and 6.0 in the cell's acidic organelles. Unlike intracellular free  $Ca^{2+}$  concentrations, which can rapidly change by perhaps 100-fold, the pH inside a cell varies by only fractions of a pH unit, and such changes may be quite slow. Although the optical change of even the best fluorescent pH probes is usually relatively small, they have proven to be effective tools for investigating the role of intracellular pH in diverse physiological and pathological processes, including cell proliferation,<sup>3</sup> apoptosis,<sup>4,5</sup> fertilization,<sup>6</sup> malignancy,<sup>7</sup> multidrug resistance,<sup>8,9</sup> ion transport,<sup>10-12</sup> lysosomal storage disorders and Alzheimer's disease.<sup>13</sup> It would be desirable to provide compounds which are effective as pH-dependent fluorescent dye indicators, particularly at low pH. To this end, Diwu and coworkers recently reported<sup>14</sup> the development and pH-dependent fluorescence of pyridyloxazole dye (PDMPO) and demonstrated its ability to selectively label acidic organelles. We herein disclose our efforts in this area, on the synthesis, structural characterization and physical properties of a class of heterocyclic betaines, pyrido[1,2-*a*]quinoxalines, which exhibit fluorescence which is sensitive to changes in pH in a relevant physiological range.

## Results and discussion

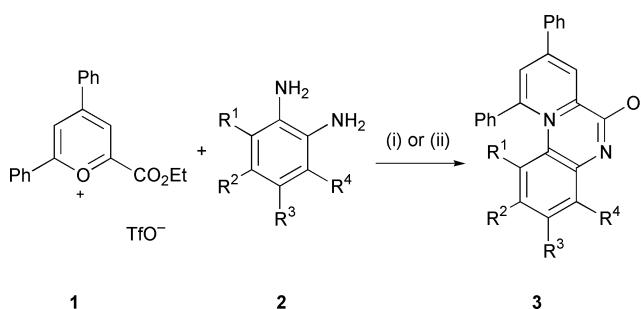
### Synthesis of pyrido[1,2-*a*]quinoxalines

The reaction of pyrylium-2-carboxylates with 1,2-phenylenediamines affords the tricyclic 6-oxidopyrido[1,2-*a*]quinoxalin-

Table 1 Pyrido[1,2-*a*]quinoxalines 3

Compound	R <sup>1</sup>	R <sup>2</sup>	R <sup>3</sup>	R <sup>4</sup>
3a	H	H	H	H
3b	H	Me	Me	H
3c	H	Cl	Cl	H
3d	H	NO <sub>2</sub>	NO <sub>2</sub>	H
3e	H	Cl	H	H
3f	H	H	Cl	H
3g	H	CF <sub>3</sub>	H	H
3h	H	H	CF <sub>3</sub>	H
3i	H	NO <sub>2</sub>	H	H
3j	H	H	NO <sub>2</sub>	H
3k	H	H	H	OH
3l	OH	H	H	H

11-ium ring system and although the UV spectrum of one analogue has been reported there has been little further study done on this interesting mesoionic heterocycle.<sup>15-17</sup> We undertook the synthesis of pyrido[1,2-*a*]quinoxalines through the reaction of various *o*-diaminoaromatics **2** with commercially available 4,6-diphenyl-2-ethoxycarbonylpyrylium triflate (**1**) (Scheme 1). We



Scheme 1 (i) AcOH, reflux; (ii) MeOH, room temp.

generally found that conducting the reaction in methanol at room temperature or refluxing acetic acid was optimal, the reaction being complete in a few hours with the triflate salt of the heterocyclic product often crystallising from the reaction medium. 4,5-Disubstituted 1,2-phenylenediamines along with 1,2-phenylenediamine itself gave single products **3a-d** (see Table 1) however 4-monosubstituted diamines **2e**, **2g** and **2i**

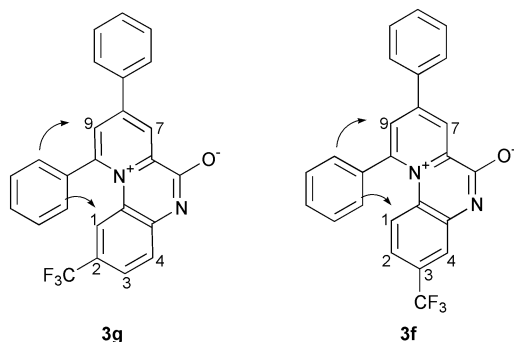
† Electronic supplementary information (ESI) available: NMR data of compounds **3a-k** and views of the crystal structures of **3g**, **3i** and **3k**. See <http://www.rsc.org/suppdata/p2/b1/b102755g/>

gave approximately 1 : 1 mixtures of the two possible regioisomers **3e,f**, **3g,h** and **3i,j** which could be readily separated by flash-chromatography to afford the neutral zwitterionic pyrido[1,2-*a*]quinoxalines. To distinguish between the two isomers a series of NOE experiments were carried out on the trifluoromethyl derivatives **3g** and **3h**.<sup>‡</sup> It was clearly demonstrated that the more polar isomer by silica gel chromatography is the 2-trifluoromethyl isomer **3g** and that this relationship held for the chloro **3e,f** and nitro **3i,j** analogues also. This assignment of isomers was subsequently validated by X-ray crystal analysis (*vide infra*). Reaction of 3-hydroxy-1,2-phenylenediamine with the pyrylium salt of **1** afforded a single isomer. This was believed to be the 4-hydroxy isomer **3k** since the 1-hydroxy isomer **3i** would contain an unfavorable steric interaction between the hydroxy group and the 10-phenyl substituent and this was subsequently confirmed by X-ray analysis of a single crystal of compound **3k**.

### X-Ray crystallography

Several of the pyrido[1,2-*a*]quinoxalines synthesized during the present study gave single crystals suitable for X-ray diffraction analysis. The crystal structures of 2-trifluoromethyl analogue **3g**, 2-nitro analogue **3i** and 4-hydroxy analog **3k** are represented in Fig. 1. Compounds **3i** and **3k** were studied as triflate salts. These structures provide conclusive confirmation of the assignment of substituent position as determined previously by NMR experiments. Structural details are similar for the three analogues. Looking at compound **3g** in more detail, the geometry of the tricyclic core is significantly distorted from that expected for a fully aromatic system. In particular, the distances around C6, 1.500(6) to C14, 1.342(5) to N5, and about N1, 1.385(5) to C10, 1.432(5) to C12, 1.373 to C14(5) are consistent with significant localization of electron density. The tricyclic pyrido[1,2-*a*]quinoxalinium system is not planar, but rather consists of two flat sections twisted at the central ring. The dihedral angle between the planes defined by rings A and C is 21.3(1)°. Phenyl ring E is rotated 53.2(1)° out of the ring C plane while phenyl ring D is rotated 20.8(1)° out of the same plane. These distortions impart a helical shape to the core of the molecule. Fig. 2 illustrates the  $\pi$ -stacking arrangement for **3g**. For the lower and middle molecules the separation between the planes defined by atoms N5, C6, O6, C14, N1, and C7 is 3.27 Å, while for the middle and upper molecules it is 3.48 Å. The  $\pi$ -stacking places the oppositely charged atoms O6 and N1 in close proximity. The relevant distances are 3.360(5) Å between those atoms in the lower pair and 3.714(5) Å in the upper two. Unlike the **3g** structure, there is no  $\pi$ -stacking arrangement for the other analogues which are cations in the crystal lattice. The intermolecular interactions for these triflate salts are dominated by hydrogen bonding contacts.

<sup>‡</sup> Saturation of the indicated protons caused NOE enhancements as shown.



**3g**  
H-1 ( $\delta$  7.45, d,  $J_{1,3}$  = 2.2 Hz)  
H-9 ( $\delta$  8.4, d,  $J_{7,9}$  = 2.6 Hz)

**3f**  
H-1 ( $\delta$  7.36, d,  $J_{1,2}$  = 9.1 Hz)  
H-9 ( $\delta$  8.44, d,  $J_{7,9}$  = 2.6 Hz)

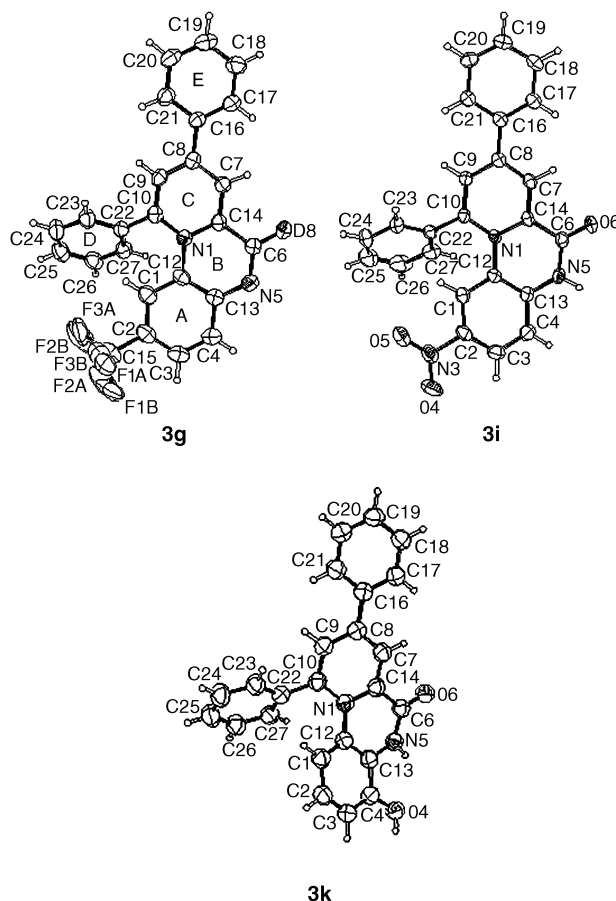


**Fig. 1** Views of **3g**, **3i** and **3k** from their crystal structures showing the numbering scheme employed. Anisotropic displacement ellipsoids for non-hydrogen atoms are shown at the 50% probability level. Hydrogen atoms are displayed with an arbitrarily small radius.

### Membrane permeability study

The permeation of selective pyridoquinoxalines through the lipid membrane was evaluated in the artificial membrane permeability model (see Experimental section for details). The permeability values for the selected compounds, shown in Table 2, fall in the range of medium ( $>10^{-6}$  cm s<sup>-1</sup>) to high ( $>10^{-5}$  cm s<sup>-1</sup>). For comparison, the permeability for Rhodamine 123 and calcein acetoxymethyl ester (calcein AM), two fluorescence probes widely used for intra-cellular microscopic imaging studies and cell-based assays,<sup>18</sup> was also determined in the artificial membrane system. The compounds of interest here all have a comparable or higher (passive) membrane permeability than that for Rhodamine 123 or calcein AM in aqueous buffer at pH 7. Most likely, these compounds would penetrate cell membrane in the time frame comparable to that for routine cellular experiments involving the rhodamine or calcein AM dye. It is beyond the scope of this study to address the issues of efflux transporters and compound stability in the biological system, both of which can affect the utilities of these compounds as intracellular pH probes.

### UV-visible spectroscopy and pK<sub>a</sub> determination

The pyrido[1,2-*a*]quinoxalines are all intensely colored and show pH-dependent color changes visible to the human eye. Table 2 lists absorption maxima and molar absorption coefficients for compounds **3** under both acidic (pH = 3.5) and basic (pH = 9.6) conditions. Shown in Fig. 3 are a series of UV-visible spectra obtained in systematically varied pH buffers, ranging from 2 to 11, for the parent compound **3a**. It is evident from the spectral changes and well-defined isosbestic points that there is only one ionization step in the observed pH range

**Table 2** Membrane permeability, UV absorption and fluorescence emission properties for selective pyridoquinoxalines compounds **3a–k**

Compound	Permeability/cm s <sup>-1</sup>	$\lambda_{\text{max}}$ ; AC (pH 3.5) <sup>b</sup>	$\lambda_{\text{max}}$ ; AC (pH 9.6)	$\lambda_{\text{em}}$ ; Rel. int. (pH 3.5) <sup>c</sup>
<b>3a</b>	$3.9 \times 10^{-6}$	344; 25000	319; 33000	566; 1.00
<b>3b</b>	$2.4 \times 10^{-5}$	333; 13000	319; 15000	565; 0.47
<b>3c</b>	Nt <sup>a</sup>	350; 20000	322; 25000	564; 0.89
<b>3d</b>	$1.7 \times 10^{-5}$	375; 20000	334; 20000	Not detected
<b>3f</b>	$5.1 \times 10^{-6}$	Nt	Nt	Nt
<b>3g</b>	$2.9 \times 10^{-5}$	353; 21000	319; 28000	553; 1.02
<b>3h</b>	$3.9 \times 10^{-6}$	351; 22000	320; 27000	554; 0.71
<b>3i</b>	$1.5 \times 10^{-5}$	333; 22000	334; 26000	567; 0.47
<b>3k</b>	$1.9 \times 10^{-5}$	343; 14000	318; 13000	474; 0.20
Rhodamine 123	$7.7 \times 10^{-6}$	Nt	Nt	Nt
Calcein AM	$4.0 \times 10^{-6}$	Nt	Nt	Nt

<sup>a</sup> Nt = not tested. <sup>b</sup>  $\lambda_{\text{max}}$  = wavelength at absorption maximum (in nm). AC = molar absorption coefficient (in cm<sup>-1</sup> M<sup>-1</sup>). <sup>c</sup>  $\lambda_{\text{em}}$  = wavelength of emission maximum (in nm, excitation at 350 nm). Rel Int = Relative Intensity with respect to compound **3a**.

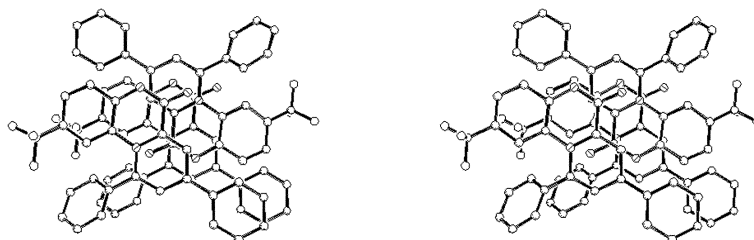


**Fig. 2** A stereo view of molecules of **3g** illustrating the  $\pi$ -stacking. The molecule in the middle of the sandwich is at symmetry position  $x,y,z$ . The one below is at symmetry position  $1-x,-y,-z$ ; above symmetry position  $-x,-y,-z$ . Hydrogen atoms are omitted for clarity.

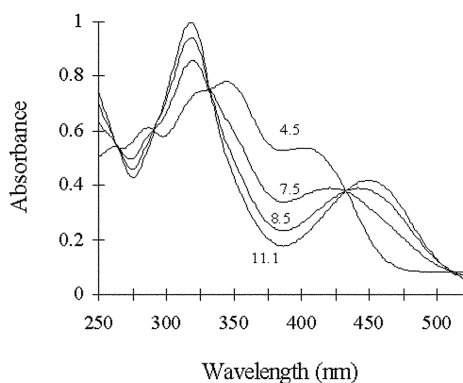


**Fig. 3** UV-visible absorption spectra of compound **3a** (36  $\mu\text{M}$ ) obtained in pH 4.5, 7.5, 8.5 and 11.1 buffers.

**Table 3** Aqueous  $\text{p}K_{\text{a}}$ 's obtained by the spectrophotometric method of Albert and Serjeant (see ref. 19)

Compound <b>3</b>	$\text{p}K_{\text{a}}$
<b>a</b>	7.4
<b>b</b>	7.5
<b>c</b>	6.3
<b>d</b>	4.5
<b>g</b>	6.5
<b>h</b>	6.6
<b>i</b>	5.9
<b>k</b>	6.9
<b>m</b>	5.1

and that both chemical forms are stable. All the compounds in Table 2 exhibit pH-dependent spectral changes, but respond quite differently in terms of the shape of the spectra and the magnitude of the change. The ionization constant can be readily estimated using the spectrophotometric  $\text{p}K_{\text{a}}$  method of Albert and Serjeant.<sup>19</sup> The results are shown in Table 3. The nature of the functional groups on the quinoxaline ring significantly affects the  $\text{p}K_{\text{a}}$  value. For example, the electron-withdrawing nitro function shifted the  $\text{p}K_{\text{a}}$  value from 7.4 for the unsubstituted parent compound **3a** to 5.9 for the mono-substituted compound **3i** and 4.5 for the di-substituted com-

ound **3d**. By manipulating the electronic property of the tricyclic ring, we have synthesized a series of novel pH-sensitive dyes covering a usable pH range from 3 to 9.

#### Fluorescence studies

Except for compound **3d**, all compounds listed in Table 1 are brightly fluorescent in acidic media with diminishing emission intensity and a small red shift toward more basic conditions. Maximum emission wavelengths and fluorescence intensities (relative to compound **3a**) for selected compounds **3** are listed in Table 2. Representative fluorescence emission spectra of compound **3a** from 450 to 700 nm at an excitation wavelength of 375 nm in pH buffers are shown in Fig. 4. The plots of peak

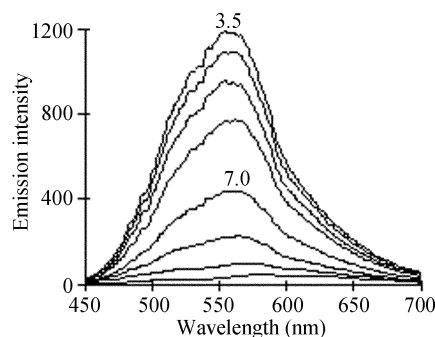


**Fig. 4** Fluorescence emission spectra of compound **3a** in (from top to bottom) pH 3.5, 4.5, 5.0, 6.5, 7.0, 7.5, 8.5 and 11.1 buffer. The excitation wavelength was at 375 nm. The intensity is in arbitrary units.

emission intensity as a function of pH (result not shown here) for the compounds in Table 1 are sigmoidal in shape with the inflection point approximately at the  $\text{p}K_{\text{a}}$  for the compound.

Of particular interest is the mono-nitro substituted compound **3i** for which selected fluorescence excitation spectra in buffers of different pH values are shown in Fig. 5. The significant red shift from acidic to basic environment allows accurate ratiometric excitation measurement. The plot of intensity ratios at 458 nm/364 nm (purposely chosen to match the wavelengths of commonly available UV and visible lasers) vs. pH's, shown in

**Table 4** Analytical data for pyrido[1,2-*a*]quinoxalines **3a–k**

Compound (Formula)	Method	Yield (%)	Mp/°C (solvent)	Found (%) (Required)		
				%C	%H	%N
<b>3a</b> (C <sub>24</sub> H <sub>16</sub> N <sub>2</sub> O·CHF <sub>3</sub> O <sub>3</sub> S·CH <sub>3</sub> OH)	A	88	206–208 (MeOH)	58.57 (58.86)	3.61 (3.99)	5.32 (5.28)
<b>3b</b> (C <sub>26</sub> H <sub>20</sub> N <sub>2</sub> O·CHF <sub>3</sub> O <sub>3</sub> S·0.75 CH <sub>2</sub> Cl <sub>2</sub> )	A	79	265–266 (MeOH–DCM)	56.40 (56.47)	4.11 (3.84)	5.07 (4.75)
<b>3c</b> (C <sub>24</sub> H <sub>14</sub> Cl <sub>2</sub> N <sub>2</sub> O·CHF <sub>3</sub> O <sub>3</sub> S)	A	84	283–285 (MeOH)	52.70 (52.92)	3.00 (2.66)	4.72 (4.94)
<b>3d</b> (C <sub>24</sub> H <sub>14</sub> N <sub>4</sub> O <sub>5</sub> ·0.5 CH <sub>3</sub> OH)	A	75	274 dec. (MeOH–Et <sub>3</sub> N)	64.72 (64.76)	3.14 (3.55)	12.25 (12.33)
<b>3e</b> (C <sub>24</sub> H <sub>15</sub> ClN <sub>2</sub> O·CH <sub>2</sub> Cl <sub>2</sub> ·0.5 CH <sub>3</sub> OH)	B	31	162 dec. <sup>a</sup> (MeOH–DCM)	63.61 (63.31)	4.23 (3.96)	6.19 (5.79)
<b>3f</b> (C <sub>24</sub> H <sub>15</sub> ClN <sub>2</sub> O·CH <sub>2</sub> Cl <sub>2</sub> )	B	36	140 dec. <sup>a</sup> (MeOH–DCM)	64.50 (64.19)	3.83 (3.66)	6.21 (5.99)
<b>3g</b> (C <sub>25</sub> H <sub>15</sub> F <sub>3</sub> N <sub>2</sub> O·2H <sub>2</sub> O)	B	27	175 dec. <sup>a</sup> (MeOH–DCM)	66.61 (66.37)	3.95 (4.23)	6.18 (6.19)
<b>3h</b> (C <sub>25</sub> H <sub>15</sub> F <sub>3</sub> N <sub>2</sub> O·CH <sub>2</sub> Cl <sub>2</sub> )	B	32	180 dec. <sup>a</sup> (MeOH–DCM)	62.63 (62.29)	3.77 (3.42)	5.77 (5.59)
<b>3i</b> (C <sub>24</sub> H <sub>15</sub> N <sub>3</sub> O <sub>3</sub> ·CHF <sub>3</sub> O <sub>3</sub> S·CH <sub>3</sub> OH·0.5 H <sub>2</sub> O)	B	46	222 dec. <sup>a</sup> (DCM–EtOAc–MeOH)	53.51 (53.43)	3.44 (3.62)	7.18 (7.19)
<b>3j</b> (C <sub>24</sub> H <sub>15</sub> N <sub>3</sub> O <sub>3</sub> ·CHF <sub>3</sub> O <sub>3</sub> S·0.5 CH <sub>3</sub> OH)	B	46	216 dec. <sup>a</sup> (DCM–EtOAc–MeOH)	54.33 (54.74)	3.46 (3.24)	7.49 (7.51)
<b>3k</b> (C <sub>24</sub> H <sub>16</sub> N <sub>2</sub> O <sub>2</sub> ·CHF <sub>3</sub> O <sub>3</sub> S·CH <sub>3</sub> OH)	A	37	272–273 (MeOH)	57.13 (57.14)	3.56 (3.87)	5.48 (5.13)

<sup>a</sup> Significant darkening up to decomposition temperature.

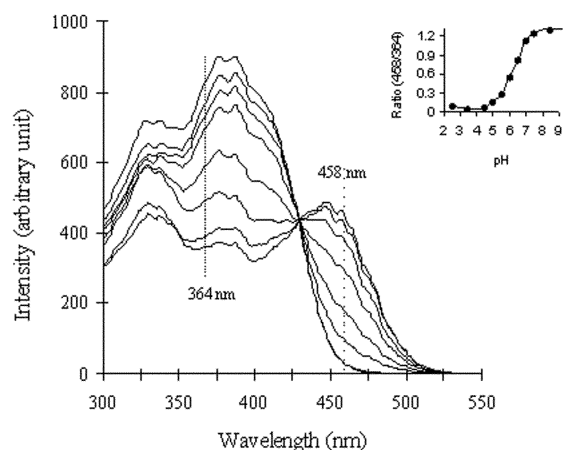


**Fig. 5** Excitation spectra of compound **3i** in (from top to bottom at 364 nm) pH 3.5, 4.5, 5.5, 6.0, 6.5, 7.0 and 8.5 buffers. The fluorescence emission was monitored at 575 nm. The inset shows the fluorescence intensity ratio at the excitation wavelength of 458 nm over 364 nm vs. pH. Note that the intensity ratio at a particular pH is not affected by the total fluorescence.

Fig. 5 (inset), indicates that the ratiometric technique is well-suited for *in situ* pH measurement in the pH 4–8 range. Compound **3i** is a better alternative to existing pH-sensitive ratioable dyes, *e.g.*, DM-NERF and di-Cl-NERF,<sup>20</sup> for applications such as confocal fluorescence microscope imaging of intra-cellular pH changes.<sup>23</sup>

## Conclusion

The most attractive feature of the use of pyrido[1,2-*a*]quinoxalines as pH-dependant fluorescent probes is their ease of synthesis (one single step from commercial reagents) particularly when compared to the multi-step preparation of the PDMPO dye mentioned previously.<sup>14</sup> Also of great value is the ability to prepare many, diverse analogs wherein tuning of the electronic properties of the tricyclic ring system is made possible by altering the nature of the attached functional groups. This can vary the pK<sub>a</sub> values for these pyrido[1,2-*a*]quinoxalines by at least three log units.

## Experimental<sup>24</sup>

### Preparation of pyrido[1,2-*a*]quinoxalines

See Table 4 for analytical data.

**Method A:** *e.g.*, preparation of 8,10-diphenyl-5,6-dihydro-6-oxopyrido[1,2-*a*]quinoxalin-11-ium **3a** trifluoromethanesulfonate. To a solution of pyrylium salt **1** (454.4 mg, 1.0 mmol)

in anhydrous methanol (8 cm<sup>3</sup>) was added 1,2-phenylenediamine (119 mg, 1.1 mmol) and the mixture was left standing for 6 days at room temperature. The resulting yellow crystals were filtered and rinsed with dichloromethane to provide pyrido[1,2-*a*]quinoxaline **3a** which was combined with a second crop obtained by dilution of the methanolic mother liquor with an equal volume of dichloromethane followed by filtration (438 mg, 88%) as a yellow solid.

**Method B:** *e.g.*, preparation of 8,10-diphenyl-6-oxido-3-trifluoromethylpyrido[1,2-*a*]quinoxalin-11-ium **3h** and 8,10-diphenyl-6-oxido-2-trifluoromethylpyrido[1,2-*a*]quinoxalin-11-ium **3g**. To a solution of pyrylium salt **1** (454.4 mg, 1.0 mmol) in anhydrous methanol (10 cm<sup>3</sup>) was added 4-trifluoromethyl-1,2-phenylenediamine (193.7 mg, 1.1 mmol) and the resulting mixture was heated at 75 °C (oil-bath temp.) for 1 h. The solvent was evaporated and the residue was purified by chromatography on silica gel with dichloromethane–ethyl acetate–methanol (9 : 9 : 2) to provide 8,10-diphenyl-5,6-dihydro-6-oxo-3-trifluoromethylpyrido[1,2-*a*]quinoxalin-11-ium **3g** (112 mg, 27%) as a red solid. Further elution with dichloromethane–ethyl acetate–methanol (9 : 9 : 2) afforded 8,10-diphenyl-5,6-dihydro-6-oxo-2-trifluoromethylpyrido[1,2-*a*]quinoxalin-11-ium **3h** (134 mg, 32%) as a red solid.

### Crystal structure determination of compound **3g**<sup>25</sup>

Crystals of **3g** were recrystallised from dichloromethane–ethyl acetate–hexanes as red needles. A single crystal (0.06 × 0.24 × 0.30 mm) was mounted in inert oil and transferred to the diffractometer.

**Crystal data.** C<sub>25</sub>H<sub>15</sub>F<sub>3</sub>N<sub>2</sub>O, *M* = 416.39, monoclinic, *a* = 7.045(3), *b* = 10.615(4), *c* = 25.694(10) Å, β = 92.68(3)°. *U* = 1919.3(13) Å<sup>3</sup>, *T* = 293(2) K, space group *P*2<sub>1</sub>/*n*, *Z* = 4, μ(Mo–Kα) = 0.917 mm<sup>-1</sup>, 3418 reflections measured, 2843 unique (*R*<sub>int</sub> = 0.090) which were used in all calculations. The final residuals were *R*<sub>1</sub> = 0.060 (2813 data; *I* > 2σ*I*) and *wR*(*F*<sup>2</sup>) = 0.241 (all data).

### Crystal structure determination of compound **3i**<sup>25</sup>

Crystals of **3i** were recrystallised from dichloromethane–ethyl acetate–methanol as yellow plates. A single crystal (1.20 × 0.50 × 0.20 mm) was mounted in inert oil and transferred to the diffractometer.

**Crystal data.** [C<sub>24</sub>H<sub>18</sub>N<sub>3</sub>O<sub>3</sub>]<sup>+</sup> [CF<sub>3</sub>SO<sub>3</sub>]<sup>-</sup> · H<sub>2</sub>O, *M* = 561.48, triclinic, *a* = 8.454(2), *b* = 9.474(2), *c* = 17.001(3) Å, α = 74.91(3), β = 85.33(3), γ = 68.33(3)°. *U* = 1221.6(4) Å<sup>3</sup>, *T* = 223(2) K, space group *P*1̄, *Z* = 2, μ(Mo–Kα) = 0.208 mm<sup>-1</sup>, 13511 reflections measured, 3303 unique (*R*<sub>int</sub> = 0.118) which were used in

all calculations. The final residuals were  $R1 = 0.071$  (2998 data;  $I > 2\sigma I$ ) and  $wR(F^2) = 0.185$  (all data).

### Crystal structure determination of compound 3k<sup>25</sup>

Crystals of **3k** were recrystallised from dichloromethane–ethyl acetate–methanol as colourless prisms. A single crystal ( $0.58 \times 0.24 \times 0.22$  mm) was mounted in inert oil and transferred to the diffractometer.

**Crystal data.**  $[C_{24}H_{17}N_2O_2]^+[CHF_3SO_3]^- \cdot CH_3OH$ ,  $M = 546.51$ , triclinic,  $a = 7.633(3)$ ,  $b = 10.495(4)$ ,  $c = 15.251(6)$  Å,  $\alpha = 98.61(3)$ ,  $\beta = 90.52(3)$ ,  $\gamma = 93.99(3)^\circ$ .  $U = 1204.8(8)$  Å<sup>3</sup>,  $T = 223(2)$  K, space group  $P\bar{1}$ ,  $Z = 2$ ,  $\mu(\text{Mo-K}\alpha) = 0.205$  mm<sup>-1</sup>, 9167 reflections measured, 4216 unique ( $R_{\text{int}} = 0.0176$ ) which were used in all calculations. The final residuals were  $R1 = 0.082$  (3587 data;  $I > 2\sigma I$ ) and  $wR(F^2) = 0.205$  (all data).

### Artificial membrane permeability assay

The artificial membrane permeability assay was developed at GlaxoSmithKline based on the classical microfiltration filter–black lipid membrane technique<sup>21</sup> and the contemporary high throughput parallel chemical analysis approach<sup>22</sup> with the underlying purpose of developing a high-throughput physico-chemical technique for evaluating drug intestinal absorption and membrane penetration. Conceptually and experimentally, the artificial phospholipid membrane technique is similar to the widely used Caco-2 cell monolayer permeation technique. In short, egg phosphatidyl choline (2%) and cholesterol (1%) are dissolved in *n*-decane. A small amount of the volatile mixture is applied to the bottom of the microfiltration filter inserts. Phosphate buffer (0.05 M, pH 7.05) is quickly added to the donors and receivers, and the lipids are allowed to form self-assembled lipid bilayers across the small holes in the filter. The permeation experiment is initiated by spiking the compounds of interest to the donor sides and the experiment is stopped at a pre-determined elapsed time. The samples are withdrawn and transferred to appropriate vials for analysis by HPLC with UV detection.

### References

- 1 H. S. Freeman and J. Sokolowska, *Rev. Prog. Color. Relat. Top.*, 1999, **29**, 8.
- 2 A. W. Czarnick, *Chem. Biol.*, 1995, **2**, 423.
- 3 E. A. Schutle, A. Hohendahl, H. Stegmann, J. R. Hirsch, H. Saleh and E. Schlatter, *Cell. Physiol. Biochem.*, 1999, **9**, 310.
- 4 D. Pérez-Sala, D. Collado-Escobar and F. Mollinedo, *J. Biol. Chem.*, 1995, **270**, 6235.
- 5 J. Li and A. Eastmann, *J. Biol. Chem.*, 1995, **270**, 3203.
- 6 K. Suzuki, Y. Tanaka, Y. Nakajima, K. Hirano, H. Itoh, H. Miyata, T. Hayakawa and K. Kinoshita, Jr., *Biophys. J.*, 1995, **68**, 739.
- 7 G. R. Martin and R. K. Jain, *Cancer Res.*, 1994, **54**, 5670.
- 8 S. Simon, D. Roy and M. Schindler, *Proc. Natl. Acad. Sci. USA*, 1994, **91**, 1128.
- 9 P. D. Poepe, Li Yong Wei, J. Cruz and D. Carlson, *Biochemistry*, 1993, **32**, 11042.
- 10 H. Zhao, X. Xu, J. Diaz and S. Muallem, *J. Biol. Chem.*, 1995, **270**, 19599.
- 11 S. A. Levine, S. K. Nath, C. H. C. Yun, J. W. Yip, M. Montrose, M. Donowitz and C. M. Tse, *J. Biol. Chem.*, 1995, **270**, 13716.
- 12 R. M. Shepherd and J.-C. Henquin, *J. Biol. Chem.*, 1995, **270**, 7915.
- 13 T. A. Davise, R. E. Fine, R. J. Johnson, C. A. Levesque, W. H. Rathbun, K. F. Seetoo, S. J. Smith, G. Strohmeier, L. Volicer, L. Delva and E. R. Simons, *Biochem. Biophys. Res. Commun.*, 1994, **194**, 537.
- 14 Z. Diwu, C.-S. Chen, C. Zhang, D. H. Klaubert and R. P. Haugland, *Chem. Biol.*, 1999, **6**, 411.
- 15 Y. P. Andreichikov, N. V. Kolovda and G. N. Dorofeenko, *Khim. Geterotsikl. Soedin.*, 1975, **11**, 1587.
- 16 L. N. Chernavskaya, N. V. Kolovda, S. G. Blagorodov and N. A. Dmitrieva, *Khim.-Farm. Zh.*, 1983, **18**, 700.
- 17 P. Molina, M. Alajarin, M. Loranzo-Pena, A. Tarraga and M. J. Vilaplana, *J. Heterocycl. Chem.*, 1984, **21**, 1609.
- 18 R. P. Haugland, *Handbook of Fluorescence Probes and Research Chemicals*, Molecular Probes, Eugene, Oregon, 1998.
- 19 A. Albert and E. P. Serjeant, *The Determination of Ionisation Constants*, Chapman and Hall, London, 1984.
- 20 R. P. Haugland, *Handbook of Fluorescence Probes and Research Chemicals*, Molecular Probes, Eugene, Oregon, 1998.
- 21 M. Thompson, R. B. Lennox and R. A. McClelland, *Anal. Chem.*, 1982, **54**, 76.
- 22 M. Kansy, F. Senner and K. Gubernator, *J. Med. Chem.*, 1998, **41**, 1007.
- 23 Both DM-NERF and di-Cl-NERF need to be excited at 488 and 514 nm for ratiometric imaging. An important logistic issue is that a confocal fluorescence system with an UV and visible laser of the appropriate wavelengths would be more readily available than a system with two Ar lasers (redundant) or 1 Ar laser with dynamic mode switching between 488 and 514 nm (technically challenging). (R. Moosher, personal communication).
- 24 A table of NMR data for compounds **3a–k** is given in the supplementary material.
- 25 Crystallographic data for compounds **3g**, **3i** and **3k** are given in the supplementary material. CCDC reference numbers 162091–162093. See <http://www.rsc.org/suppdata/p2/b1/b102755g/> for crystallographic files in .cif or other electronic format.